

## Enhancing energy and exergy efficiency of pyramid solar still through nanoparticle integration: a comparative analysis

Malik Yousef Al-Abed Allah

Department of Mechanical Engineering, College of Engineering, King Fahd University of Petroleum and Minerals (KFUPM), Dhahran, Saudi Arabia, email: alabdullhm@gmail.com

Received 5 September 2023; Accepted 3 December 2023

---

### ABSTRACT

This paper compares the efficiency and thermal performance of regular pyramid solar stills to those modified with silica or aluminum oxide nanoparticles. The amount of exergy lost by the pyramid solar still's various parts has been estimated, studied, and discussed. The exergy of evaporation is greater at the improved solar stills, and evaporation occurs at a faster rate. Also, compared to regular stills, the upgraded ones have higher energy and exergy efficiency. The impact of varying factors on the performance of solar stills is briefly discussed as well. Maximum energy efficiency for mixes of aluminum oxide and water is 55.29% and for mixtures of silica oxide and water is 41.38%, whereas for the typical still it is just 35.68%. In addition, conventional stills, stills based on silica oxide nanoparticles, and aluminum oxide all had exergy efficiencies of 11.48% or lower throughout the day.

*Keywords:* Pyramid solar still; Exergy; Nanoparticles; Energy efficiency; Productivity; Desalination

---

### 1. Introduction

As a result of rising population levels and increased levels of water pollution, there is currently a severe shortage of clean water across the world. This has been a driving force behind the development of a variety of technologies for the desalination of brackish water and seawater to keep up with the rising demand for freshwater. The use of solar energy to power the desalination process in arid regions that have an abundance of solar resources has been suggested as one of the best possible solutions [1]. Due to the ease with which they can be assembled and put into operation; solar stills have become the solar desalination technology that is most used in remote areas. Conventional solar stills are comprised mostly of a water basin and a transparent cover, both of which are simple components that may be simply built using materials that are easily accessible in the area [2].

Several different cover configurations for solar stills have been suggested to improve the productivity of solar

stills, the most prevalent of which are single-slope [3], double-slope [4], tubular [5], and triangular [6] coverings. The poor productivity of solar stills continues to be the primary obstacle in the widespread use of these devices, despite the many improvements that have been made to the geometry of these devices. As a result, more sophisticated solar stills, such as those with exterior reflectors [7] and multi-stage systems [8] amongst others, are now being developed to maximize the production of freshwater.

The heat transfer mechanism and operating temperature are the two most influential factors on the yield of a solar still. By improving the thermal characteristics of the base water, the coefficient of heat transmission can be increased. Suspending nanoparticles in the base fluid is a simple technique that improves the thermal property and, consequently, productivity. The formation of nanofluid involves suspending nanoparticles in a base fluid.

Solar still technology that employs nanoparticles has the ability to enhance the thermal properties of basin

water. This is owing to the fact that nanoparticles have different properties from the basic liquid, such as high solar absorption and superior thermal conductivity [9,10]. Consequently, it will contribute to an enhancement in the thermal system's performance. When nanoparticles are combined with a base fluid, there are two basic techniques for enhancing heat transmission:

- To enhance the nanoparticle concentration in the base fluid, which will ultimately result in a faster rate of heat transfer.
- The collisions between nanoparticles and the molecules of the base fluid occur first, while the collisions of the particles with the solar still are wall result in a rise in energy.

Eastman et al. [11] measured the thermal conductivity of water containing 5% copper oxide nanoparticles. The authors discovered that water's thermal conductivity was 60% greater than that of pure water. Similarly, the thermal conductivity of water containing 5% aluminum nanoparticles was 40% greater than that of pure water.

Experiments conducted by Xie et al. [12] to measure the thermal conductivity of nanofluids containing aluminum nanoparticles ranging in size from 12.2 to 304 nm reveal an inverse relationship between thermal conductivity and particle size, except for the biggest particles.

In a comprehensive investigation conducted by Abdelgaied et al. [13] the performance of a hemispheric solar still (HSS) was examined under various modification scenarios, including the use of CuO nanofluid (CuO-NF), phase change material (PCM), and a combination of both CuO-NF and PCM. The findings revealed noteworthy distinctions in performance among these modifications. Specifically, the HSS enhanced with CuO-NF demonstrated superior performance compared to the HSS employing PCM alone. However, the most remarkable outcomes were observed in the HSS where both CuO-NF and PCM were combined. In this configuration, the yield and efficiency of the HSS were notably improved, achieving values of 8.65 L/m<sup>2</sup> and 63.61%, respectively. Notably, this innovative combination of CuO-NF and PCM also led to a substantial reduction in cost, amounting to merely 0.00654 \$/L, thereby signifying a remarkable 75% cost reduction when juxtaposed with conventional HSS configurations. These findings underscore the considerable potential of CuO-NF and PCM integration in enhancing the performance and cost-efficiency of hemispheric solar stills, holding significant implications for sustainable desalination technologies.

Moreover, in a scholarly endeavor Attia et al. [14] conducted an extensive thermo-economic investigation was undertaken to evaluate diverse hemispheric solar still (HSS) designs from the perspectives of energy, exergy, and cost considerations. The study encompassed the utilization of various materials in these designs, leading to notable and acceptable enhancements in performance. Specifically, the use of rubber material yielded improvements ranging from 14.29% to 46.94%, while the incorporation of a wick material resulted in enhancements between 12.24% and 40.81%. It is important to highlight that these improvements were

achieved while maintaining the production rate of the distillation process unaltered. This study serves as a significant contribution to the field of HSS design and performance optimization, shedding light on the potential for substantial efficiency gains through material selection and design considerations.

Additionally, Sharshir et al. [15] conducted a detailed assessment of hemispherical solar still (HSS) performance with various modifications, comparing it to a standard HSS configuration. Four distinct cases of enhancement were explored, including alterations involving phase change materials (PCM) and nanofluids. The results revealed substantial performance improvements when using sheep fat as a PCM, with impressive enhancements in daily yield, thermal efficiency, and exergy efficiency. Additionally, the introduction of graphite nanofluid further boosted these indicators. The replacement of conventional PCM with nano-based PCM, combined with other modifications, led to nearly 100% improvements in all performance metrics. Notably, these enhancements occurred despite the introduction of additional material costs. Furthermore, the HSS system contributed to carbon mitigation through reduced CO<sub>2</sub> emissions, earning a carbon credit. Overall, this study demonstrated the potential for enhancing HSS efficiency and economic viability through material and configuration modifications.

The objective of the current study is to examine the effects of nanoparticles on the energy efficiency, exergy efficiency, and exergy destruction of pyramid solar still components (basin, glazier, and water) with and without nanoparticles. The exergy of evaporation and productivity of a modified solar still (with silica SiO<sub>2</sub> or aluminum oxide Al<sub>2</sub>O<sub>3</sub> nanoparticles) vs. a conventional one is explored. Using nanoparticles to increase the diurnal exergy efficiencies of the solar still components, that is, the basin liner, the glazier cover, and the saline water, is also described.

## 2. Experimental setup and devices

The present study focuses on the investigation of the design, fabrication, and construction of a pyramid solar still, with particular attention given to its performance in generating distilled water. Thermocouples are employed to measure the temperatures of the basin water, glass, and vapor, while hourly solar radiation and ambient temperature data are obtained from the PV project at Jordan University of Science and Technology.

A glass cover, an interior galvanized iron sheet, insulation, and an external galvanized iron sheet compose the pyramid solar still. The glass cover is 6 mm thick, and each glass plate has a width of 60 cm, a height of 25 cm, and a sloping angle of 30°. Internal galvanized iron sheets with a thickness of 1.25 mm were welded together to form a closed box with a base area (absorber area) of 0.36 m<sup>2</sup> (0.6 m × 0.6 m) and a height of 25 cm. In addition, external galvanized iron sheets with a thickness of 0.9 mm were bonded together to produce an outer surface with a base area of 0.49 m<sup>2</sup> (0.7 m × 0.7 m), a height of 30 and 5 cm of polystyrene insulation in between.

The solar pyramid still deployed in the experiment is depicted in Fig. 1.

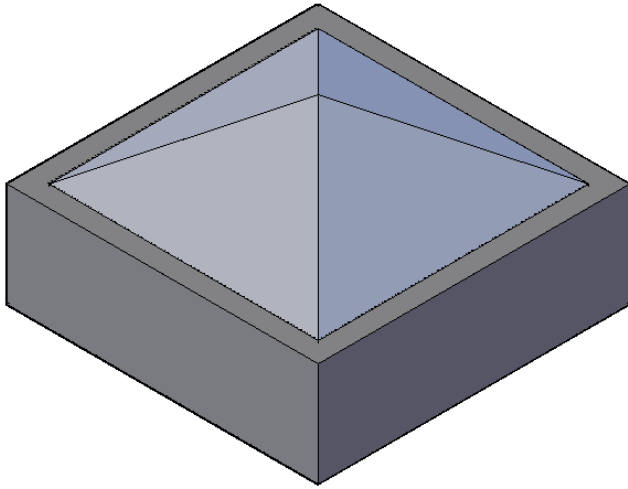


Fig. 1. 3D model for pyramid solar still.

### 3. Exergy balance equations

Exergy is dissipated or lost ( $Ex_d$ ) due to the irreversibility of the process or its components ( $Ex_g$ ). The exergy balance for a system or its constituents can be derived by integrating the principles of energy conservation and the non-conservation of exergy.

Fig. 2 depicts the exergy flow schematic of the passive solar still. Assuming that the heat capacity of the basin-liner, glass cover, and insulating materials is insignificant, the exergy balancing equations of the three main components of the solar still are shown here, excluding exergy accumulation in the components.

#### 3.1. Basin-liner

The passive solar basin-liner still absorbs the portion of solar exergy ( $Ex_{sun}$ ) reaching it. A portion of this, that is, the useable exergy ( $Ex_w$ ), is used to heat the salt water, while some are lost through insulation ( $Ex_{insu}$ ) and the remainder is lost ( $Ex_{d,b}$ ) [16].

$$Ex_{d,b} = (\tau_g \tau_w \alpha_b) Ex_{sun} - (Ex_w + Ex_{insu}) \quad (1)$$

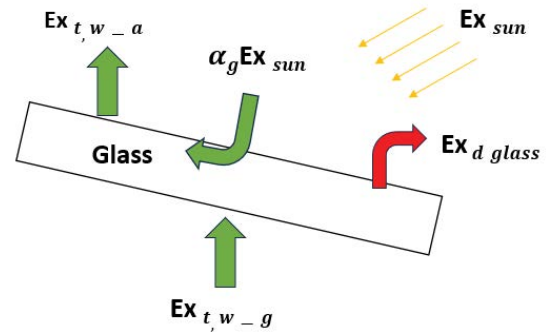
where  $\tau_g$ ,  $\tau_w$ , and  $\alpha_b$  are the transmittance of the glass cover, the transmittance of the saline water, and the absorptivity of the basin-liner, respectively.

Exergy of the solar radiation on the solar still per unit area,  $Ex_{sun}$  (in  $W/m^2$ ), is given as:

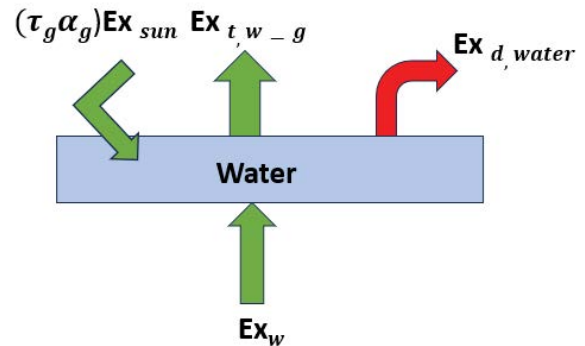
$$Ex_{sun} = G_s \left[ 1 + \frac{1}{3} \left( \frac{T_a}{T_s} \right)^4 - \frac{4}{3} \left( \frac{T_a}{T_s} \right) \right] \quad (2)$$

$$Ex_w = h_w (T_b - T_w) \left( 1 - \frac{T_a}{T_b} \right) \quad (3)$$

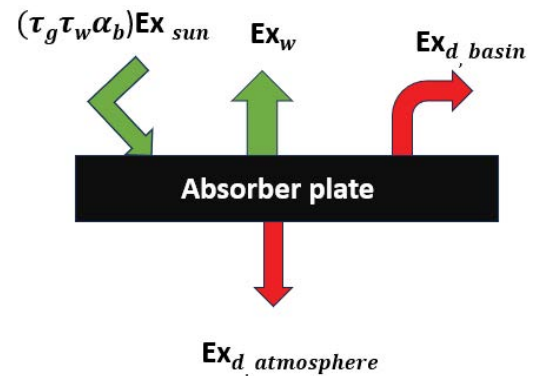
where  $h_w$  is the convective heat transfer coefficient between basin-liner and saline water ( $W/m^2 \cdot K$ ).



(a): Exergy balance on the glass.



(b): Exergy balance on the water.



(c): Exergy balance on the basin.

Fig. 2. Illustrates exergy transfers within a horizontal, single-effect, basin-type passive solar still. (a) Depicts the exergy balance on the glass cover. (b) Shows the exergy balance of the body of water. (c) Represents the exergy equilibrium on the basin lining.

$$Ex_{insu} = h_b (T_b - T_a) \left( 1 - \frac{T_a}{T_b} \right) \quad (4)$$

where  $h_b$  is the overall heat transfer coefficient between basin-liner and atmosphere ( $W/m^2 \cdot K$ ).

### 3.2. Saline water

The exergy input to the bulk of salt water in the basin can be expressed as the sum of two components: the proportion of incoming solar exergy absorbed by water, denoted as  $(\tau_g \alpha_w) Ex_{sun}$ , and the usable exergy derived from the basin-liner, denoted as  $Ex_w$ . A fraction of the total energy is allocated to the exergy associated with the heat transfer occurring between the surface of the salt water and the glass cover present in the solar still, denoted as  $Ex_{t,wg}$ . The remaining energy is dissipated and considered as lost, referred to as  $Ex_{d,w}$ .

$$Ex_{d,w} = (\tau_g \alpha_w) Ex_{sun} + Ex_w - Ex_{t,wg} \quad (5)$$

where  $\alpha_w$  is the absorptivity of saline water and  $Ex_{t,wg}$  is the exergy associated with the heat transfer through evaporation ( $Ex_{e,w-g}$ ), radiation ( $Ex_{r,w-g}$ ) and convection ( $Ex_{c,w-g}$ ) between the saline water surface and the glass cover inside the solar still and is calculated:

$$Ex_{r,w-g} = Ex_{e,w-g} + Ex_{c,w-g} - Ex_{c,w-g} \quad (6)$$

$$Ex_{e,w-g} = h_{e,w-g} (T_w - T_{gi}) \left( 1 - \frac{T_a}{T_w} \right) \quad (7)$$

where  $h_{e,w-g}$  is the evaporative heat transfer coefficient between saline water and glass cover ( $W/m^2 \cdot K$ ).

$$Ex_{c,w-g} = h_{c,w-g} (T_w - T_{gi}) \left( 1 - \frac{T_a}{T_w} \right) \quad (8)$$

where  $h_{c,w-g}$  is the convective heat transfer coefficient between saline water and glass cover ( $W/m^2 \cdot K$ ).

$$Ex_{r,w-g} = h_{r,w-g} (T_w - T_{gi}) \left[ 1 + \frac{1}{3} \left( \frac{T_a}{T_w} \right)^4 - \frac{4}{3} \left( \frac{T_a}{T_w} \right) \right] \quad (9)$$

where  $h_{r,w-g}$  is the radiative heat transfer coefficient between saline water and glass cover ( $W/m^2 \cdot K$ ).

### 3.3. Glass cover

$$Ex_{d,g} = \alpha_g Ex_{sun} + Ex_{t,wg} - Ex_{t,g-a} \quad (10)$$

The symbol  $\alpha_g$  represents the absorptivity of the glass cover, while  $Ex_{t,g-a}$  denotes the exergy loss resulting from heat losses from the glass cover to the environment due to radiation ( $Ex_{r,g-a}$ ) and convection ( $Ex_{c,g-a}$ ). This expression can be expressed as:

$$Ex_{t,g-a} = Ex_{r,g-a} + Ex_{c,g-a} \quad (11)$$

$$Ex_{r,g-a} = h_{r,g-a} (T_{go} - T_a) \left[ 1 + \frac{1}{3} \left( \frac{T_a}{T_{go}} \right)^4 - \frac{4}{3} \left( \frac{T_a}{T_{go}} \right) \right] \quad (12)$$

where  $h_{r,g-a}$  is the radiative heat transfer coefficient between glass cover and atmosphere ( $W/m^2 \cdot K$ ).

$$Ex_{c,g-a} = h_{c,g-a} (T_{go} - T_a) \left( 1 - \frac{T_a}{T_{go}} \right) \quad (13)$$

where  $h_{c,g-a}$  is the convective heat transfer coefficient between glass cover and atmosphere ( $W/m^2 \cdot K$ ).

## 4. Energy and exergy efficiency of solar still

The evaluation of solar still performance often relies on energy efficiency, which is widely regarded as a crucial criterion [17].

The total efficiency is found by adding up the hourly yield times the latent heat of evaporation split by the average daily sunshine on the whole surface of the device.

$$\eta = \frac{\sum m_{ew} \times h_{ig}}{\sum I(t) \times A_s \times 3600} \quad (14)$$

In the previous work [17], researchers gave the balance equations of exergy for the three main parts of the solar still: the basin liner, the salt water, and the glazier cover. Assuming that the heat capacity of the materials used to make the parts is small, the buildup of exergy could be ignored. Exergy analysis, which is based on the second rule of thermodynamics, shows how good the energy is. The exergy analysis is a strong way to find out what is wrong with a system, where it is wrong, and how bad it is. It also gives a precise way to measure how close the SS is to the ideal. The exergy efficiency of a solar still is the measure of the energy that comes out of the water that has been distilled to the energy that comes in from the sun.

$$\eta_{EX} = \frac{\text{Exergy output of solar still}}{\text{Exergy input of solar still}} = \frac{Ex_{evap}}{Ex_{input}} \quad (15)$$

In a solar still, energy is made when salty water evaporates and then condenses back into a liquid. In real life, some of the water that evaporates and condenses on the cover drips back into the basin. Because of this, the amount of exergy measured from the experimental results would be less than the amount predicted by theory. A solar still's hourly exergy output can be written as [17]:

$$Ex_{output} = Ex_{evap} = \frac{m_{ew} \times h_{ig}}{(3600s \cdot h^{-1})} \times \left( 1 - \frac{T_a}{T_w} \right) \quad (16)$$

where  $m_{ew}$  is the hourly yield of solar still (kg/h),  $h_{ig}$  is the latent heat (J/kg),  $T_a$  is the surrounding air temperature ( $^{\circ}C$ ), and  $T_w$  is the basin water temperature ( $^{\circ}C$ ).

The exergy input to solar through radiation  $x$  sun  $E$  can be expressed in terms of insolation [17]:

$$Ex_{sun} = A_s \times I(t)_s \left[ 1 + \frac{1}{3} \left( \frac{T_a}{T_s} \right)^4 - \frac{4}{3} \left( \frac{T_a}{T_s} \right) \right] \quad (17)$$

where  $A_s$  is the area of the basin in ( $m^2$ ),  $I(t)_s$  is the insolation on the inclined glazier surface of the solar still ( $W/m^2$ ) and  $T_s$  is the sun temperature (6,000 K).

### 5. Results and discussion

#### 5.1. Material used in experiment

In this study, a tripartite experimental investigation was conducted. The initial phase involved the utilization of silica oxide nanoparticles ( $SiO_2$ ) in conjunction with water (nanofluid) within the solar still. The subsequent phase replicated the methodology of the first group but substituted silica oxide nanoparticles ( $SiO_2$ ) with aluminum oxide nanoparticles ( $Al_2O_3$ ). It is noteworthy that the water depth inside the still remained constant at 2.7 cm throughout these experiments. Finally, the third phase was executed without the introduction of any nanoparticles. Detailed specifications for the silica and aluminum oxide nanoparticles can be found in Table 1.

#### 5.2. Solar radiation and temperatures

Experiments were conducted on days characterized by clear skies and closely matched solar radiation levels, aimed at providing a comprehensive comprehension of solar still performance across a spectrum of water depths, ranging from 2.7 cm. The diurnal variations in solar radiation, ambient temperature, glass temperature, and water basin temperature for the three distinct scenarios are graphically depicted in Figs. 3–5. Throughout the course of the day, solar radiation and all temperature metrics exhibited an ascending

trend, reaching their zenith at 14:00 p.m. Subsequently, a reversal in this trend was observed, with a gradual decline in values occurring until sunset.

For the solar still configuration devoid of nanoparticles, the maximum recorded temperatures were 67.8°C, 52.9°C, and 31.58°C at 14:00 p.m. for the water basin, glass surface, and ambient environment, respectively. Concurrently, the solar radiation value reached 985.7  $W/m^2$  during this time period.

#### 5.3. Energy efficiency

Fig. 6 shows the energy efficiency of the pyramid solar still with time for the three considered cases calculated using Eq. (14). Energy efficiency strictly depends on water

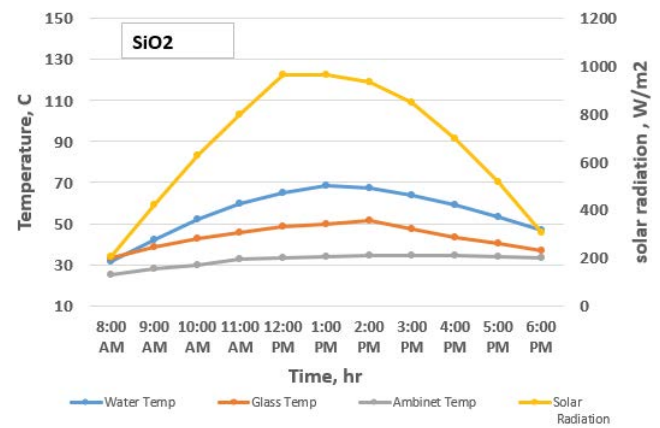


Fig. 4. Daily variations of temperature and solar intensity of the still with  $SiO_2$  nano.

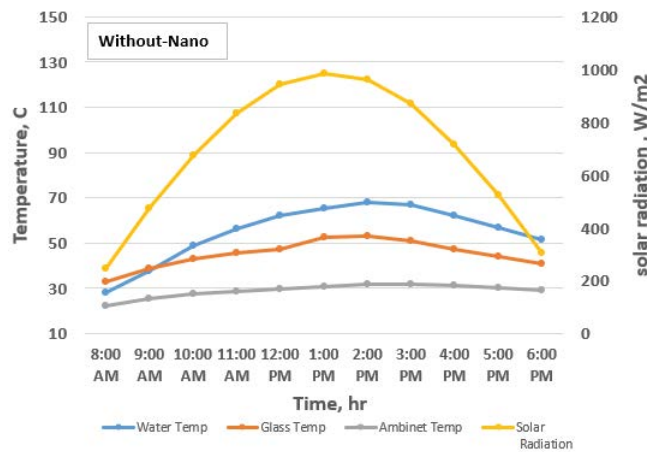


Fig. 3. Daily variations of temperature and solar intensity of the still without nano.

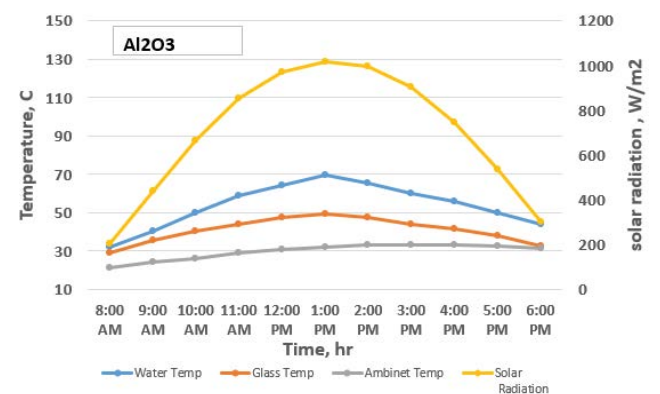


Fig. 5. Daily variations of temperature and solar intensity of the still with  $Al_2O_3$  nano.

Table 1  
Specifications of silica and aluminum oxides nanoparticles

Material	Chemical symbol	Specific heat ( $J/kg \cdot K$ )	Density ( $kg/m^3$ )	Thermal conductivity ( $W/m \cdot K$ )	Average particle size (nm)
Aluminum oxide	$Al_2O_3$	773	3,900	46	10–14
Silica oxide	$SiO_2$	800	2,530	1.4	10–14

productivity and solar radiation. As the basin’s water temperature reduces, the evaporation rate declines, and therefore the energy efficiency decreases. The increase in energy efficiency with silica oxide nanoparticles SiO<sub>2</sub> is about 8.56% and about 11.78% with Al<sub>2</sub>O<sub>3</sub> nanoparticles, compared to the still without nanoparticles.

5.4. Input, output exergy rates, and exergy efficiency

Based on Eqs. (16) and (17), the hourly input and output exergy rates are depicted in Fig. 7. It is depicted that the output exergy rates increase when solar radiation increases. the output exergy rates for solar still with Al<sub>2</sub>O<sub>3</sub> and SiO<sub>2</sub> increase away from the output exergy rate obtained at solar still without nanoparticles of water. The output exergy increased by about 5.2% and 14.5%, respectively, compared to the solar still without nanoparticles during the day.

Fig. 8 presents the temporal evolution of exergy efficiencies across the three examined scenarios. Broadly, a discernible pattern emerges in which the exergy efficiency exhibits a progressive increase commencing from 10:00 a.m. and culminating at its zenith around 2:00 p.m. The highest recorded exergy efficiencies among the three cases are approximately 20.73% for aluminum oxide nanoparticles (Al<sub>2</sub>O<sub>3</sub>), 19.6% for silica oxide nanoparticles (SiO<sub>2</sub>), and 18.1%

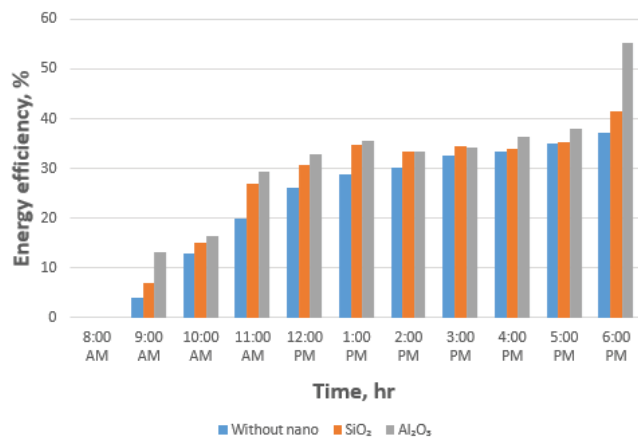


Fig. 6. Energy efficiency with respect to time.

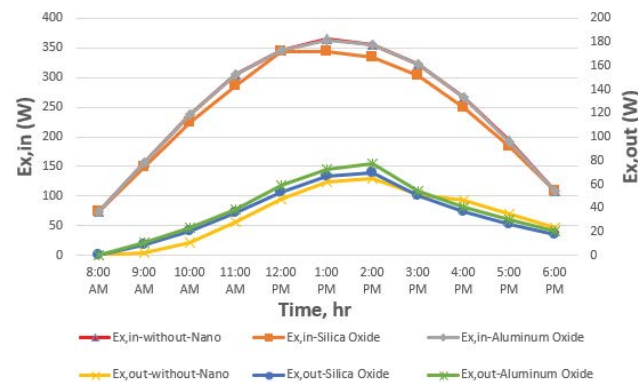


Fig. 7. Hourly input and output exergy rates with respect to time.

for the configuration devoid of nanoparticles. However, by approximately 3:00 p.m., a reversal in the exergy efficiency trends becomes evident.

Notably, the solar still devoid of nanoparticles consistently registers higher exergy efficiencies than the nanoparticle-enhanced counterparts. This intriguing observation can be attributed to the intrinsic energy storage capacity of the water residing within the basin, which promotes an escalated rate of evaporation and consequently augments exergy production. This phenomenon underscores the intricate interplay between nanoparticle additives, water depth, and the overall exergy efficiency performance in the solar still system.

5.5. Accumulative freshwater produced and exergy destruction

The comparison between the accumulative amounts of freshwater produced by the pyramid solar still with and without using any nanoparticles is shown in Fig. 9. As time progresses, water production from the solar still without nanoparticles increases until they achieve the maximum values (178 mL) at 2:00 PM. Then, the behavior is reversed, and they gradually decrease until sunset.

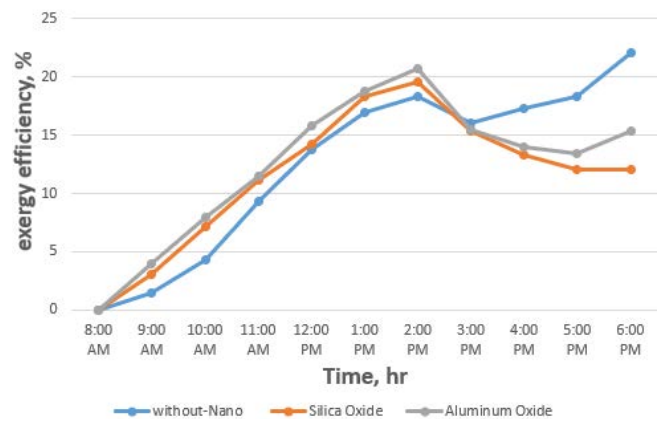


Fig. 8. Hourly input and output exergy rates with respect to time.

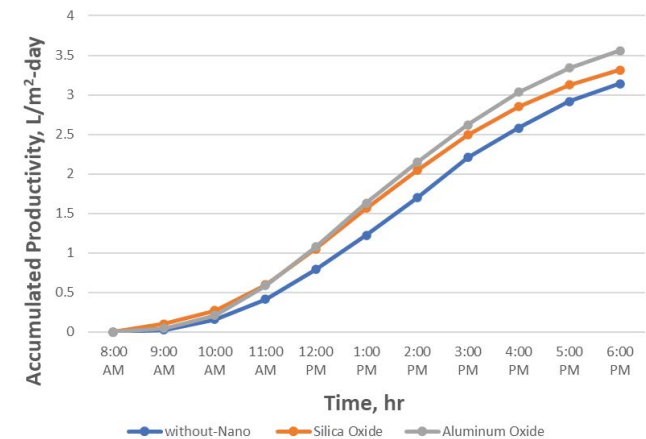


Fig. 9. Accumulated water productivity with respect to time from the three considered cases of the still.

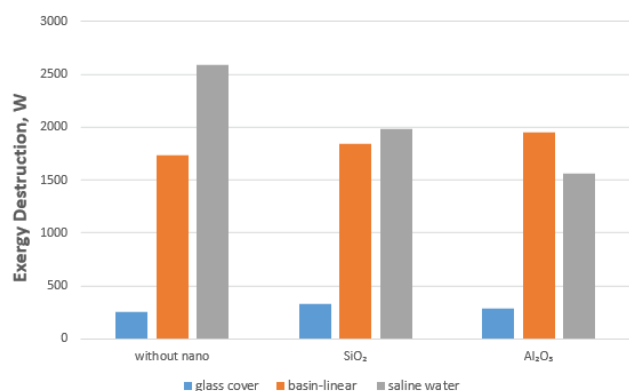


Fig. 10. Exergy destruction in the basin liner, the glass cover, and the saline water.

As a result, the accumulated productivity is found to be 3.14 L/m<sup>2</sup>-d. Adding nanoparticles to the water caused an increase in hourly water productivity of up to 20.26% when using silica oxide SiO<sub>2</sub> (from 8:00 AM to 2:00 PM) and an increase of up to 5.5% (from 3:00 PM to 6:00 PM). While adding aluminum oxide nanoparticles Al<sub>2</sub>O<sub>3</sub> caused an increase in hourly water productivity by up to 26.3%, (from 8:00 AM to 2:00 PM) and an increase of 14% (from 3:00 PM to 6:00 PM). For SiO<sub>2</sub> and Al<sub>2</sub>O<sub>3</sub>, the accumulated productivity is found to be 3.31 and 3.56 L/m<sup>2</sup>-d.

Through exergy analysis, the amount and location of exergy loss can be determined. Consequently, exergy efficiency would be improved by implementing applicable measures and decreasing exergy waste. The rate of instantaneous exergy destruction was determined for various components of the pyramid solar still, including the basin liner, saline water, and glazing cover, with and without nanoparticles.

Fig. 10 depicts the variation of exergy destruction in basin liners depending on hourly intervals. Maximum daily exergy destruction of 1,731 W in basin liner without nanoparticle addition. In addition, as depicted in the figure, the exergy destruction of the basin liner of the pyramid solar still with aluminum oxide nanoparticles Al<sub>2</sub>O<sub>3</sub> was slightly greater than that of the conventional still due to the lowest temperature difference between the basin liner and water ( $T_b - T_w$ ) in the modified pyramid solar still as compared to the conventional.

Exergy destruction in the basin liner varied hourly, as illustrated in Fig. 10. The basin liner achieved the highest daily exergy destruction (1,731 W) without the use of nanoparticles. Furthermore, the lowest temperature difference between the basin liner and the water ( $T_b - T_w$ ) in the modified pyramid solar still was a little bit larger than that of conventional still, as shown in that figure.

Fig. 10 displays that the lowest exergy destruction was achieved in the salt water. An increase in the temperature difference between the surface of the salty water and the inside surface of the glass was found to reduce the exergy destruction in the saline water ( $T_w - T_{gs}$ ). Since the temperature difference between the saline water with nanoparticles and the still without nanoparticles was greater in the former scenario, the exergy degradation of the former

was less. Therefore, the modified pyramid solar still had a higher evaporation rate than the conventional still.

## 6. Conclusion

In conclusion, this research conducted an extensive assessment of the pyramid solar stills, both in their conventional form and when modified with aluminum oxide and silica oxide nanoparticles. The main findings of this study indicate:

- Introduction of nanoparticles enhances the energy efficiency and energy output of the pyramid solar stills.
- The basin component is identified as the primary source of exergy destruction, emphasizing the importance of selecting appropriate materials for insulation and the basin liner to reduce exergy losses.
- The application of aluminum oxide and silica oxide nanoparticles results in significantly higher energy and exergy efficiencies in the modified solar stills.
- Maximum energy efficiency was observed for mixtures containing nanoparticles, notably 55.29% for aluminum oxide and 41.38% for silica oxide, whereas conventional stills achieved only 35.68%.
- The study highlights the significant advantages of incorporating nanoparticles in pyramid solar stills to improve their overall thermal performance and efficiency.

These results underscore the potential for enhancing the efficiency of pyramid solar stills through nanoparticle modifications, which can contribute to more sustainable and effective water desalination systems in arid regions.

## References

- [1] M.T. Ali, H.E.S. Fath, P.R. Armstrong, A comprehensive techno-economical review of indirect solar desalination, *Renewable Sustainable Energy Rev.*, 15 (2011) 4187–4199.
- [2] S. Rashidi, N. Rahbar, M.S. Valipour, J.A. Esfahani, Enhancement of solar still by reticular porous media: experimental investigation with exergy and economic analysis, *Appl. Therm. Eng.*, 130 (2018) 1341–1348.
- [3] S. Rashidi, M. Bovand, J. Abolfazli Esfahani, Optimization of partitioning inside a single slope solar still for performance improvement, *Desalination*, 395 (2016) 79–91.
- [4] N. Rahbar, A. Gharaiian, S. Rashidi, Exergy and economic analysis for a double slope solar still equipped by thermoelectric heating modules - an experimental investigation, *Desalination*, 420 (2017) 106–113.
- [5] G. Xie, L. Sun, Z. Mo, H. Liu, M. Du, Conceptual design and experimental investigation involving a modular desalination system composed of arrayed tubular solar stills, *Appl. Energy*, 179 (2016) 972–984.
- [6] A. Ahsan, M. Intiaz, U.A. Thomas, M. Azmi, A. Rahman, N.N. Nik Daud, Parameters affecting the performance of a low cost solar still, *Appl. Energy*, 114 (2014) 924–930.
- [7] C.-H. Huang, T.-R. Chang, Determination of optimal inclination function for external reflector of basin type still for maximum distillate productivity, *Energy*, 141 (2017) 1728–1736.
- [8] G. Xie, W. Chen, T. Yan, J. Tang, H. Liu, S. Cao, Three-effect tubular solar desalination system with vacuum operation under actual weather conditions, *Energy Convers. Manage.*, 205 (2020) 112371, doi: 10.1016/j.enconman.2019.112371.
- [9] Y. Yang, Z. George Zhang, E.A. Grulke, W.B. Anderson, G. Wu, Heat transfer properties of nanoparticle-in-fluid dispersions (nanofluids) in laminar flow, *Int. J. Heat Mass Transfer*, 48 (2005) 1107–1116.

- [10] M. Mehrali, E. Sadeghinezhad, M.A. Rosen, S.T. Latibari, M. Mehrali, H.S.C. Metselaar, S.N. Kazi, Effect of specific surface area on convective heat transfer of graphene nanoplatelet aqueous nanofluids, *Exp. Therm. Fluid Sci.*, 68 (2015) 100–108.
- [11] J.A. Eastman, U.S. Choi, S. Li, L.J. Thompson, S. Lee, Enhanced thermal conductivity through the development of nanofluids, *MRS Online Proc. Lib.*, 457 (1996) 3–11.
- [12] H. Xie, J. Wang, T. Xi, Y. Liu, F. Ai, Q. Wu, Thermal conductivity enhancement of suspensions containing nanosized alumina particles, *J. Appl. Phys.*, 91 (2002) 4568–4572.
- [13] M. Abdelgaied, M. El Hadi Attia, A.E. Kabeel, M.E. Zayed, Improving the thermo-economic performance of hemispherical solar distiller using copper oxide nanofluids and phase change materials: experimental and theoretical investigation, *Sol. Energy Mater. Sol. Cells*, 238 (2022) 111596, doi: 10.1016/j.solmat.2022.111596.
- [14] M. El Hadi Attia, A.K. Hussein, G. Radhakrishnan, S. Vaithilingam, O. Younis, N. Akkurt, Energy, exergy and cost analysis of different hemispherical solar distillers: a comparative study, *Sol. Energy Mater. Sol. Cells*, 252 (2023) 112187, doi: 10.1016/j.solmat.2023.112187.
- [15] S.W. Sharshir, M.A. Omara, A. Joseph, A.W. Kandeal, A.M. Elsaid, E.M.S. El-Said, I. Alatawi, M. Elashmawy, G.B. Abdelaziz, Thermoenviroeconomic performance augmentation of solar desalination unit integrated with wick, nanofluid, and different nano-based energy storage materials, *Sol. Energy*, 262 (2023) 111896, doi: 10.1016/j.solener.2023.111896.
- [16] K.R. Ranjan, S.C. Kaushik, N.L. Panwar, Energy and exergy analysis of passive solar distillation systems, *Int. J. Low-Carbon Technol.*, 11 (2016) 211–221.
- [17] S.W. Sharshir, A.H. Elsheikh, G. Peng, N. Yang, M.O.A. El-Samadony, A.E. Kabeel, Thermal performance and exergy analysis of solar stills – a review, *Renewable Sustainable Energy Rev.*, 73 (2017) 521–544.